

Compression of positron clouds using rotating wall electric fields

Dirk Peter van der Werf · Christopher Aled Isaac ·
Christopher John Baker · Timothy Mortensen ·
Michael Charlton

© Springer Science+Business Media B.V. 2011

Abstract An asymmetric dipolar rotating electric field can be used to compress a trapped cloud of positrons when applied with a frequency close that of their axial bounce, and in the presence of a low pressure molecular gas to provide cooling. Measurements of the compression rate and associated parameters are presented and compared with results of a theory we have developed. The latter treats positron behaviour in a perfect Penning trap potential, in the presence of the rotating field, with the cooling modelled in the Stokes viscous drag approximation. Good agreement between the theory and experiment has been found, which has allowed us to identify the phenomenon as a new form of sideband cooling.

Keywords Positron · Compression · Rotating wall · Penning trap

1 Introduction

The manipulation of clouds of low energy positrons has found many recent applications in fundamental physics, including antihydrogen formation [1, 2] and trapping [3], and the observation of the positronium molecule [4]. It is possible to accumulate positrons at a sufficiently high density, n_e , and at a low enough temperature, T_e , that they form a single component plasma (see e.g. [5]). This occurs when the Debye screening length, $\lambda_D = (k_B T_e \epsilon_0 / n_e q^2)^{1/2} \approx 69 (T_e / n_e)^{1/2}$ m, with T_e in degrees Kelvin and n_e in m^{-3} , is much less than the smallest plasma dimension. With the latter usually of order 1 mm, this is readily achieved with $T_e \leq 100$ K and $n_e \geq 10^{13} \text{m}^{-3}$, which are parameters typical of antihydrogen experimentation. The properties of single component plasmas have been studied extensively, and an authoritative review has been given by Dubin and O'Neil [6].

D. P. van der Werf (✉) · C. A. Isaac · C. J. Baker · T. Mortensen · M. Charlton
Physics Department, Swansea University, Swansea SA2 8PP, UK
e-mail: D.P.van.der.Werf@Swansea.ac.uk

The positron plasmas are typically held in Penning, or Penning-Malmberg, traps consisting of a series of electrically biased cylindrical electrodes arranged along the axis of a solenoid which provides a magnetic field, $\mathbf{B} = B\hat{\mathbf{z}}$, of strength in the Tesla region. The electrical potential provides axial confinement for the positrons, with the radial confinement ensured by the magnetic field; there is also an important (radial) self electric field from the plasma, which in the case of a long spheroid is given by $\mathbf{E} = n_e q \mathbf{r} / (2\epsilon_0)$, with q the charge of the positron. The positrons undergo cyclotron motion, with an angular frequency very close to the magnetic field-only value of $\Omega_c = qB/m$, and perform an axial bounce with a frequency given by $\omega_z = (2qV_0/(mz_0^2))^{1/2}$, where V_0 and z_0 are trap parameters related to the geometry and applied voltages in the pure Penning trap case (see e.g. [7]). In the crossed electric and magnetic fields the plasma also performs a magnetron type drift (actually a rotation akin to that of a solid object) with angular frequency, $\omega_D = n_e q / (2\epsilon_0 B)$.

If a rotating wall potential, typically producing a time-varying dipolar or quadrupolar electric field, is applied to the plasma in the same sense as the natural rotation, then it has been found that the radial extent of the plasma can be controlled. This so-called rotating wall technique was first developed for ions [8] and electrons [9]. More recently, this technique has been applied over a broad range of frequencies to electron and positron plasmas in a so-called strong drive regime in which the final density of the plasma is fixed by the applied frequency [10, 11]. Application of the rotating electric fields will heat the plasmas, and to counteract this a source of cooling must be provided, typically via the emission of cyclotron radiation in the high magnetic field of the trap. If this is not available (as is the case in the present study), cooling can be achieved by collisions with an added gas.

For single charged particles, or clouds in the independent particle (i.e. non-plasma) regime, several groups have achieved axialisation using sideband excitation, following the seminal work of Wineland and Dehmelt [12]. The sidebands were excited by superimposing an *oscillating* azimuthal quadrupolar electric field of the form $\cos(\omega t)$, with ω close to one of the natural frequencies of the system, onto the static trap fields. Cooling is also necessary in this technique and has been achieved using a variety of methods, dependent upon experimental circumstances [7, 13–15].

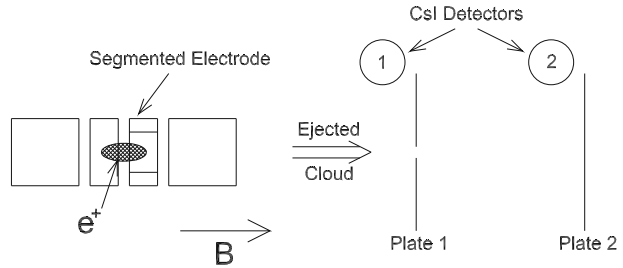
It was until recently thought that the *rotating* wall technique was only applicable to plasmas, however cloud compression in the independent particle limit has now been achieved [16, 17]. These experiments found that the highest central density of positrons occurred close to ω_z , prompting a tentative identification [17] of bounce resonance transport as the likely cause of the phenomenon. The results of the experimental and theoretical analysis we present below has shown that this is not true and that a new, and potentially important, form of sideband cooling is responsible.

The rest of the article is organised as follows. The next section contains experimental details and an outline of the theory. Results are presented in Section 3, followed by a summary and outlook in Section 4.

2 Experimental and theoretical details

Positron compression experiments were performed in a two-stage accumulator apparatus, in conjunction with a low energy positron beam [18]. Accumulation was

Fig. 1 Schematic of the second stage of the positron accumulator, illustrating the segmented electrode, and the plate system used to derive the radius of the ejected positron cloud



achieved in a Penning-Malmberg trap in the presence of molecular nitrogen buffer gas at a pressure around 6×10^{-4} mbar. Collisions involving excitation of the N_2 resulted in kinetic energy loss, whilst the positrons performed a single pass to-and-fro in the trap, thus promoting capture. Further collisions resulted in the positrons residing in a potential minimum provided by a series of cylindrical electrodes which formed the second stage of the accumulator (see Fig. 1). One of the 49 mm long electrodes was split into two with one of the halves segmented azimuthally into four parts. An external synthesiser arrangement was used to provide voltages with a phase difference of $\pi/2$ between successive segments to create the desired rotating electric field.

Though N_2 is an excellent gas to achieve efficient capture into the accumulator (due to a large cross section for positron impact excitation close to threshold at around 8.8 eV [19]), it has long been known as a poor positron cooler [20, 21]. Thus, no compression is achieved by application of the rotating wall to positrons with only the N_2 present: indeed, the positrons are sufficiently heated in this case to be lost from the trap, probably via positronium formation. Fortunately, efficient cooling can be provided by a number of other molecular gases [20, 21], with SF_6 being a convenient choice [16, 17, 20]. In our case this gas was admitted near the second stage of the accumulator at various pressures in the 10^{-5} mbar range.

The studies reported here adhered to a cycle involving: (i) accumulation for 100 ms, resulting in a cloud containing around 10^4 positrons, followed by (ii) rotating wall compression for a time, t_c , which could be varied as desired, before (iii) the cloud was ejected for measurement. An important parameter (see below) was the radius of the cloud. We were able to monitor this using a phosphor screen/external camera arrangement, but this proved to be time-consuming. Thus, a technique was developed to extract the radius which allowed measurements to be taken rapidly as the frequency of the rotating wall was varied. The method relies upon the fact that the magnetron radii of particles in a thermal cloud have a Gaussian distribution. Thus, as long as the cyclotron orbit is small when compared with that of the magnetron motion, as is true in our case, the radial profile of an ejected cloud is Gaussian. This assumption was validated in separate experiments using images from the aforementioned phosphor screen arrangement.

The measurement system is illustrated in Fig. 1. The ejected cloud must interact with two metal plates inserted into its path. The first has an on-axis hole of radius $r_0 = 1$ mm such that positrons (numbered N_1) with radii larger than this annihilate on the plate, whilst the remainder, N_2 , pass through to annihilate on the second plate. Calibrated CsI scintillator gamma-ray detectors view both plates and provide values

for N_1 and N_2 . It can be shown [22] that the width, σ , of the Gaussian profile can be derived using N_1 , N_2 and r_0 as:

$$\sigma = \frac{r_0}{\sqrt{2 \ln(1 + N_2/N_1)}}. \quad (1)$$

The ideal electrical potential experienced by a positron in a Penning trap with an added asymmetric rotating wall, with the latter having an angular frequency ω_r , and where a is proportional to the amplitude of the voltage, can be expressed as,

$$\phi(z, r, \theta) = \frac{m \omega_z^2}{q} \left(z^2 - \frac{r^2}{2} \right) + \frac{m}{q} a z r \cos(\theta + \omega_r t). \quad (2)$$

This equation can be used to compute an electric field, which together with the magnetic field, \mathbf{B} , can be used to generate equations of motion using the Lorentz force, $\mathbf{F} = q(\mathbf{E} + \mathbf{v} \times \mathbf{B})$, which are given in Cartesian coordinates by,

$$\begin{aligned} \ddot{x} &= \frac{\omega_z^2}{2} x - a z \cos(\omega_r t) + \Omega_c \dot{y} - \kappa \dot{x}, \\ \ddot{y} &= \frac{\omega_z^2}{2} y + a z \sin(\omega_r t) - \Omega_c \dot{x} - \kappa \dot{y}, \\ \ddot{z} &= -\omega_z^2 z - a(x \cos(\omega_r t) - y \sin(\omega_r t)) - \kappa \dot{z}. \end{aligned} \quad (3)$$

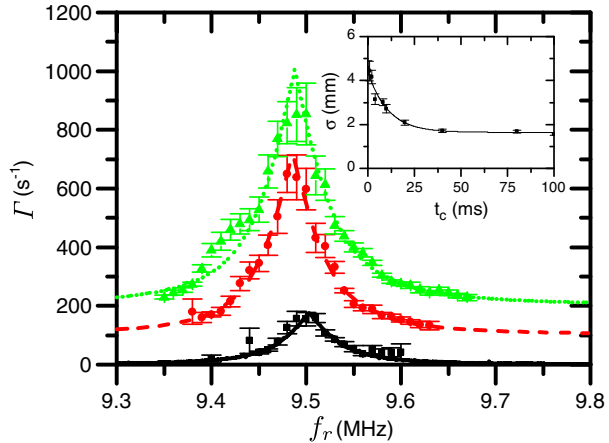
Here the cooling is described by introducing a Stokes viscous drag term with friction coefficient, κ . These equations can be expressed in a new coordinate system (see e.g. [7]) defined by $\mathbf{V}^\pm = \dot{\mathbf{r}} + \omega_\mp \hat{\mathbf{z}} \times \mathbf{r}$, (where $\mathbf{r} = x\hat{\mathbf{x}} + y\hat{\mathbf{y}}$) which decouples the magnetron and cyclotron motions. (We note that the angular frequencies for these two radial motions are related by $\omega_\pm = \frac{1}{2}(\Omega_c \pm \sqrt{\Omega_c^2 - 2\omega_z^2})$, where the $+$ and $-$ refer to the cyclotron and magnetron components, respectively.) The resulting equations can be simplified by noting: (i) that ω_r , which turns out to be centred on $(\omega_z + \omega_-)$, is far from $\Omega_c \approx \omega_+$, so the cyclotron motion is decoupled and relevant terms can be dropped, and (ii) the friction in the axial direction is much larger than experienced by the magnetron motion, so all but one friction term can be neglected. The final equations are then;

$$\begin{aligned} \dot{V}_x^- &= \omega_- V_y^- - a z \cos(\omega_r t), \\ \dot{V}_y^- &= -\omega_- V_x^- + a z \sin(\omega_r t), \\ \ddot{z} &= -\omega_z^2 z - \kappa \dot{z} - a \frac{(V_y^- \cos(\omega_r t) + V_x^- \sin(\omega_r t))}{\omega_+ - \omega_-}. \end{aligned} \quad (4)$$

These equations can be solved analytically [23] to reveal that the positrons should exponentially approach the z -axis with a compression rate, Γ , given by:

$$\Gamma = \frac{\kappa}{4} \left(1 - \sqrt{\frac{(\omega_r - \omega_0)^2}{\delta^2 + (\omega_r - \omega_0)^2}} \right), \quad (5)$$

Fig. 2 Compression rate as a function of the rotating wall frequency for amplitudes of 75 mV (■), 150 mV (●), offset by 100 s^{-1} and 225 mV (▲), offset by 200 s^{-1} . The lines are fitted using (5). *Inset:* ejected cloud radius versus the rotating wall on-time, the line is a fit to $\sigma(t)$ (see text). The uncertainties on the points in both graphs are due to scatter on repeated measurements



where the central frequency is $\omega_0 = \omega_z + \omega_-$ and the response width, δ , depends upon the applied rotating wall amplitude via,

$$\delta = \frac{a}{\sqrt{(\omega_+ - \omega_-)\omega_z}}. \tag{6}$$

Equations (5) and (6) make predictions that can be tested by experiment, as we now discuss.

3 Results

The radius of the ejected cloud (σ) was measured as described above for various compression times, t_c , and the inset of Fig. 2 shows a typical set of measurements. It is notable that, rather than approaching zero at long times, the cloud tends to a minimum size, presumably as a result of a competing expansion effect caused, for instance, by gas collisions or the presence of trap field asymmetries [24, 25]. By assuming this occurs at a constant rate γ , the data were fitted using $\sigma(t) = (\sigma_0 - \gamma/\Gamma) \exp(-\Gamma t) + \gamma/\Gamma$, where σ_0 is the width of the cloud before application of the rotating wall. Figure 2 also shows the compression rates extracted from the exponential fit as the rotating wall frequency, f_r is scanned around $f_z + f_-$. The solid lines are fits to (5) and display very good agreement.

Measurements were performed for amplitudes up to 0.6 V, and the derived values for δ from the fits are plotted in Fig. 3, with the data fitted well by the straight line (see (6)), but with an offset. From (2), it can be shown that the applied rotating wall peak-to-peak voltage, V_r , is related to a by $(m/q)af$, where f is a geometrical trap factor. The latter can be estimated by approximating the electrical potential in the trap using two first order (in r and z) Taylor expansions to yield a value of $\sim 61\text{ kHzV}^{-1}$ for comparison with the fitted gradient of $134 \pm 15\text{ kHzV}^{-1}$. It turns out that the offset and higher than expected gradient present in the data in Fig. 3 may be attributed to the anharmonicity of the well used in our experiments [23].

Fig. 3 Frequency response width versus the applied rotating wall amplitude. The *inset* shows that the central frequency of the response curve, $f_0 = \omega_0/2\pi$, remains more or less constant across this range of amplitudes with a mean value of 9.4889 ± 0.0030 MHz, which is in excellent agreement with a calculated value of 9.49 MHz using our parameters. The uncertainties are from the fits to (5) and (6)

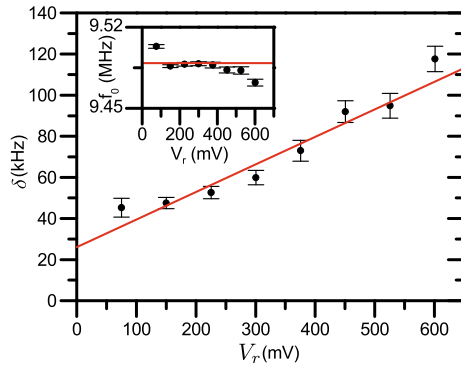


Fig. 4 Friction coefficient versus SF₆ pressure for rotating wall amplitudes 150 mV (■) and 225 mV (●)

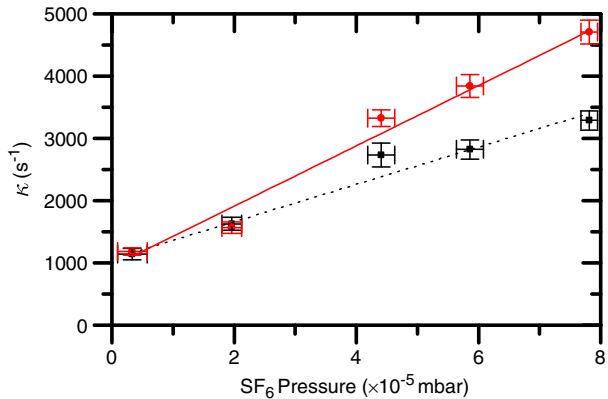
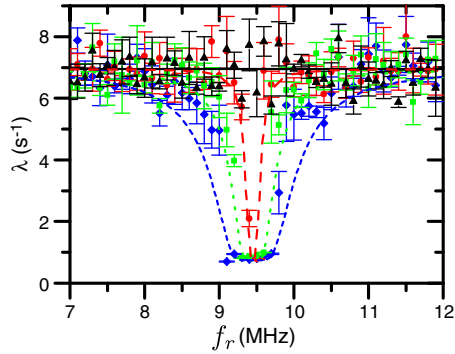


Figure 4 shows the friction coefficient, κ , versus SF₆ pressure for two different rotating wall amplitudes, indicating a linear relationship characteristic of a viscous friction model. However, there is an offset in this graph as, below a certain SF₆ pressure, the cooling is insufficient to prevent energy gain of the positrons which results in their loss from the trap. We have observed this loss in several experiments with no SF₆ in the trap. The linear behaviour with pressure may be fortuitous as the cooling is provided by low energy inelastic scattering (involving vibrational excitations) of the positrons from SF₆, and the cross section for this is known to be strongly energy dependent near threshold [19]. Thus, the temperature of the positrons (and hence κ) will depend upon the gas pressure and the drive amplitude, perhaps in a complex fashion. At least, as shown in Fig. 4, over most of the restricted range investigated to date, κ is proportional to pressure. In this respect it is also noteworthy that κ varies with the amplitude of the rotating wall voltage and for amplitudes in the range 0.06–0.60 V values spanning 500–5000 s⁻¹ have been found. This can be compared with a positron cooling time of 0.36 s measured at a pressure of 2×10^{-8} mbar [20], which at 1×10^{-5} mbar implies a cooling rate of $\sim 1,400$ s⁻¹, in acceptable accord with the extracted values.

In addition to the measurements described above, we have also performed experiments with the rotating wall present during the accumulation cycle. Whilst this mode of operation is ill-suited to the study of the compression mechanism, it

Fig. 5 The measured loss rate from the trap with the rotating wall applied during the accumulation cycle as f_r is varied at fixed SF₆ pressure, and for various amplitudes: 0 V (▲); 100 mV (●); 500 mV (■); 1.0 V (◆)



is useful from a practical point of view. In addition to annihilation on the N₂ and SF₆ gases in the second stage of the accumulator, positron loss can occur via collision-induced cross-magnetic field transport to the electrode walls. The latter effect can be minimised if the rotating wall is present during accumulation, as illustrated in Fig. 5. The loss rate, $\lambda(f_r)$, curves broaden as the applied amplitude increases, but drop around the resonance frequency to a common minimum rate, denoted by λ_0 . The curves are adequately described by the equation,

$$\lambda(f_r) = \Lambda \exp(-\Gamma(f_r)\tau_0) + \lambda_0, \tag{7}$$

where $\Lambda + \lambda_0$ is the loss rate without rotating wall, and λ_0 can be identified as the loss due to gas annihilation. It has been argued elsewhere [22] that the λ_0 value found is plausible, given the known gas pressures and annihilation parameters [26]. It is notable that the values of $\Gamma(f_r)$ are those found from the fits to (5), examples of which are shown in Fig. 2. Further work is necessary to interpret the time parameter, τ_0 . However, it is clear that this technique minimises wall loss of positrons, such that the accumulator output is not only physically narrower, but contains more positrons (by a factor of $(\Lambda + \lambda_0)/\lambda_0$) and as such is highly beneficial for experiments using extracted pulses or beams.

4 Summary and outlook

Compression of a cloud of positrons in the independent particle regime has been achieved using an asymmetric dipolar rotating field. A theoretical analysis of this effect, in an ideal Penning trap and with a Stokes approximation for the friction, has shown that it is a new form of sideband cooling. Importantly, the rotating nature of the field, rather than the oscillating excitations which have mostly been used previously, resulted in only one of the sidebands near ω_z being active. This circumvents the need for the use of narrow resonances to achieve cooling and makes the methodology applicable to a variety of useful trap/accumulator geometries and to produce higher brightness positron beams. The width of the response curve has a weak dependence upon q/m as $\delta \propto (q/m)^{1/4}$, which may allow the technique to be applied to a variety of species.

Acknowledgements We are grateful to Dr Rod Greaves of First Point Scientific Inc. for numerous helpful discussions. We thank the EPSRC for their support, currently via awards EP/E048951/1 and EP/H026932/1 and via studentships to CJB and CAI. We thank SJ Kerrigan and PR Watkeys for their help with earlier experiments and the technical staff of the Physics Department. DPvdW is grateful to RCUK for the provision of a Fellowship.

References

1. Amoretti, M., et al.: *Nature* **419**, 456 (2002)
2. Gabrielse, G., et al.: *Phys. Rev. Lett.* **89**, 213401 (2002)
3. Andresen, G.B., et al.: *Nature* **468**, 673 (2010)
4. Cassidy, D.B., Mills A.P., Jr.: *Nature* **449**, 195 (2007)
5. Jørgensen, L.V., et al.: *Phys. Rev. Lett.* **95**, 025002 (2005)
6. Dubin, D.H.E., O'Neil, T.M.: *Rev. Mod. Phys.* **71**, 87 (1999)
7. Brown, L.S., Gabrielse, G.: *Rev. Mod. Phys.* **58**, 233 (1986)
8. Huang, X.P., Anderegg, F., Hollmann, E., Driscoll, C., O'Neil, T.: *Phys. Rev. Lett.* **78**, 875 (1997)
9. Anderegg, F., Hollmann, E.M., Driscoll, C.F.: *Phys. Rev. Lett.* **81**, 4875 (1998)
10. Danielson, J.R., Surko, C.M.: *Phys. Rev. Lett.* **94**, 035001 (2005)
11. Danielson, J.R., Surko, C.M., O'Neil, T.M.: *Phys. Rev. Lett.* **99**, 135005 (2007)
12. Wineland, D., Dehmelt, H.: *Int. J. Mass Spectrom. Ion Process.* **16**, 338 (1974)
13. Savard, G.: et al.: *Phys. Lett. A* **158**, 247 (1991)
14. Powell, H.F., Segal, D.M., Thompson, R.C.: *Phys. Rev. Lett.* **89**, 093003 (2002)
15. Kellerbauer, A., et al.: *Phys. Rev. A* **73**, 062508 (2006)
16. Cassidy, D.B., Deng, S.H.M., Greaves, R.G., Mills, A.P., Jr.: *Rev. Sci. Instrum.* **77**, 073106 (2006)
17. Greaves, R.G., Moxom, J.M.: *Phys. Plasmas* **15**, 072304 (2008)
18. Clarke, J., et al.: *Rev. Sci. Instrum.* **77**, 063302 (2006)
19. Surko, C.M., Gribakin, G.F., Buckman, S.J.: *J. Phys. B At. Mol. Opt. Phys.* **38**, R57 (2005)
20. Greaves, R.G., Surko, C.M.: *Phys. Rev. Lett.* **85**, 1883 (2000)
21. Al-Qaradawi, I., Charlton, M., Borozan, I., Whitehead, R.: *J. Phys. B At. Mol. Opt. Phys.* **33**, 2725 (2000)
22. Isaac, C.A.: Axialisation of Particles in a Penning-type Trap by the Application of a Rotating Dipole Electric Field and its Application to Positron Accumulation. Swansea University (2011)
23. Isaac, C.A., Baker, C.J., Mortensen, T., van der Werf, D.P., Charlton, M.: *Phys. Rev. Lett.* **107**, 033201 (2011)
24. Malmberg, J.H., Driscoll, C.F.: *Phys. Rev. Lett.* **44**, 654 (1980)
25. Notte, J., Fajans, J.: *Phys. Plasmas* **1**, 1123 (1994)
26. Charlton, M., Humberston, J.W.: *Positron Physics*. Cambridge University Press (2001)